The shapes of cooperatively rearranging regions in glass-forming liquids

JACOB D. STEVENSON[1]*, JÖRG SCHMALIAN[2] AND PETER G. WOLYNES[1]*

[1]Department of Physics and Department of Chemistry and Biochemistry, University of California, San Diego, La Jolla, California 92093, USA
[2]Department of Physics and Astronomy and Ames Laboratory, Iowa State University, Ames, Iowa 50011, USA
*e-mail: jstevens@physics.ucsd.edu; pwolynes@ucsd.edu

Published online: 26 March 2006; doi:10.1038/nphys261

The cooperative rearrangement of groups of many molecules has long been thought to underlie the dramatic slowing of liquid dynamics on cooling towards the glassy state. For instance, there exists experimental evidence for cooperatively rearranging regions (CRRs) on the nanometre length scale near the glass transition. The random first-order transition (RFOT) theory of glasses predicts that, near the glass-transition temperature, these regions are compact, but computer simulations and experiments on colloids suggest CRRs are string-like. Here, we present a microscopic theory within the framework of RFOT, which unites the two situations. We show that the shapes of CRRs in glassy liquids should change from being compact at low temperatures to fractal or 'stringy' as the dynamical crossover temperature from activated to collisional transport is approached from below. This theory predicts a correlation of the ratio of the dynamical crossover temperature to the laboratory glass-transition temperature, and the heat-capacity discontinuity at the glass transition. The predicted correlation quantitatively agrees with experimental results for 21 materials.

The RFOT theory of glasses, based on a secure statistical mechanical formulation at the mean-field level[1–8] explains the dynamics of supercooled liquids through the existence of compact, dynamically reconfiguring regions ('entropic droplets')[9–11] whose predicted size is very much consistent with that measured (125–200 molecules), using both optical methods[12], scanning microscopy[13,14] and nuclear magnetic resonance techniques[15,16], at temperatures near the glass transition (T_g). Computer simulations[17–20] and light-microscopy studies of colloidal glasses[21] have revealed cooperatively rearranging regions (CRRs) that are not compact, contain fewer particles, and are described as 'fractal[22]' or as being 'string'-like[18,19]. In this paper, we will show that the fractal nature of the dynamically reconfiguring regions in the relatively high-temperature regime probed in current computer simulations follows quite naturally from random first-order transition (RFOT) theory. The CRRs are compact near the laboratory glass transitions, whereas RFOT theory predicts that strings will dominate near the higher dynamical crossover temperature, T_A, above which motions are no longer activated. This morphological transformation is shown in Fig. 1.

Computer simulations are carried out near the dynamical crossover. Likewise, colloidal glasses are inevitably studied near the dynamic crossover because the large size of colloidal particles, in molecular terms, means that their nanoscale constituents intrinsically move more slowly than small molecules do.

According to our theory, the dynamical crossover from activated motion has a spinodal character[3,23]. An analogous change of morphology predicted for nucleation clusters is thought to occur in ordinary first-order transitions[24], so others have already suggested that the dynamical heterogeneities near T_A should be fractal[25]. The RFOT theory predicts the temperature range where the metamorphosis from compact to fractal happens for glassy liquids. RFOT theory predicts the gap between T_A and T_g for molecular liquids should correlate inversely with the configurational heat capacity, as is found experimentally.

The mean-field theory of RFOT theory starts by constructing aperiodic minima of a free-energy functional[1] based on spatially varying density[1,26–28]. These aperiodic free-energy minima resemble the 'inherent structures' that are minima of the potential energy[29].

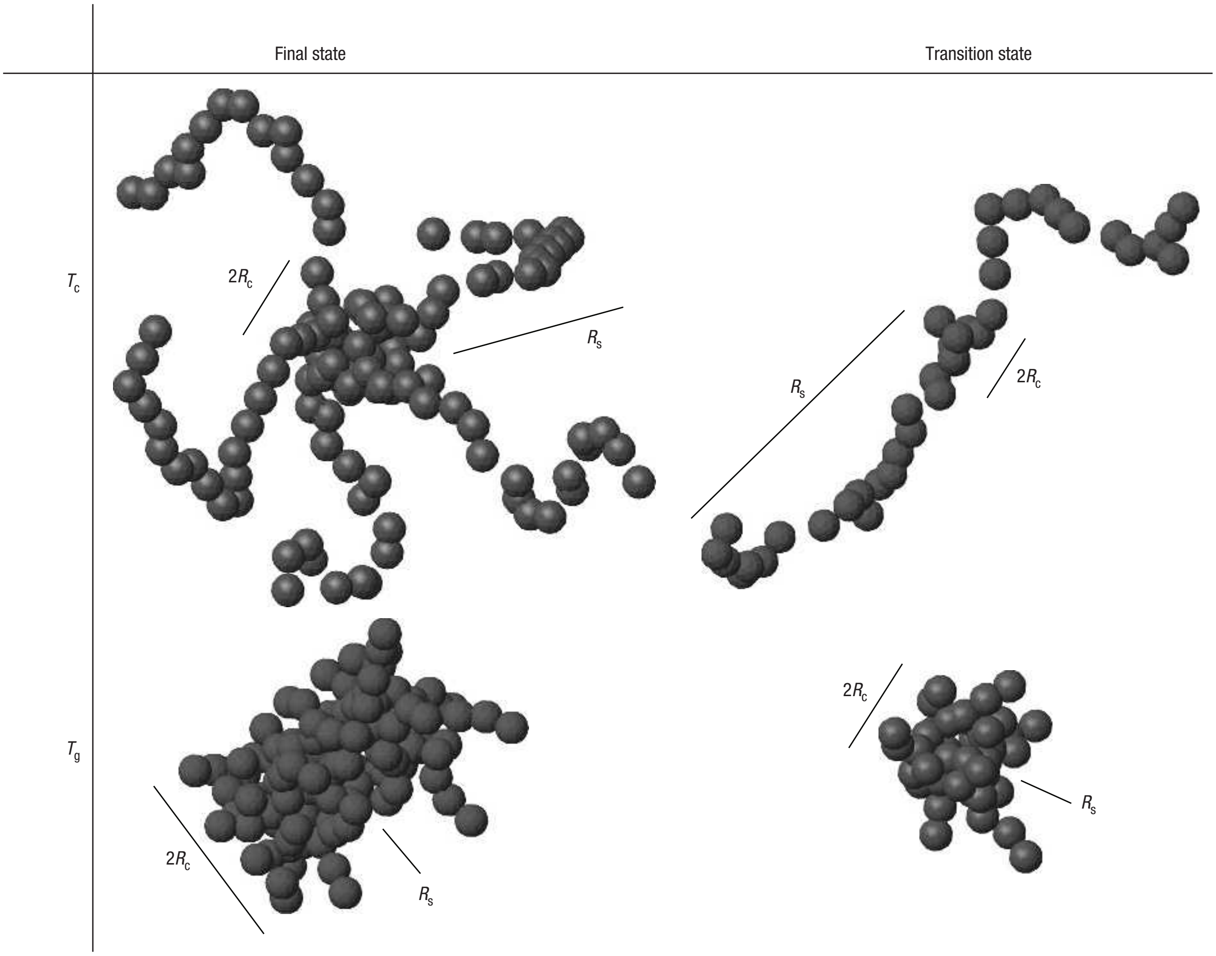

Figure 1 The shape of CRRs at T_g and T_c. The schematic appearance of the reconfiguring regions predicted by RFOT theory according to the free-energy profiles of the fuzzy-sphere model (see text) at T_g, and the crossover transition temperature T_c^{string}. The shapes are shown for both the rearranged CRR (the final state) and the partially rearranged transition state. The radius of the core, R_c, and the radius of the stringy halo, R_s, are shown in the figure.

At finite temperature, these aperiodic structures represent a compromise between the cost of localizing a particle TS_{loc} and the free-energy gain realized by particles being able to avoid each other once localized. The latter free-energy contribution is represented by an interaction term in the usual free-energy density functional. Any resulting localized, non-crystalline solution is only metastable. The difference in the free energy of the typical localized solution and the uniform state is the configurational entropy multiplied by the absolute temperature[5].

To estimate the interactions, it was pointed out[10] that, at the Kauzmann temperature T_K where the configurational entropy vanishes, their total must equal the localization cost $T_K S_{\text{loc}}$. Therefore, if a typical molecule has z nearest neighbours, a local interaction of pairs must contribute a term $v_{\text{int}} = (1/z) T_K S_{\text{loc}}$ on average. The localization entropy cost, in the free-energy functional, depends logarithmically on the amount of space each molecule moves in while encaged: $S_{\text{loc}} = (3/2) k_B \log(\alpha_L/\pi e)$, where k_B is the Boltzmann constant and α_L is the inverse square of the Lindemann ratio of the root-mean-square vibrational amplitude in the glass to the intermolecular spacing. The Lindemann ratio is predicted by detailed microscopic calculations[1,26,30], and agrees with neutron scattering measurements of the long-time plateau of the structure function. The ratio only weakly depends on the intermolecular potential and is of the order $1/10$ near T_g. Thus v_{int} should be nearly the same in units of $k_B T_K$ for all molecular glass formers made of spherical particles. This near universality of the interaction per molecular unit allows RFOT theory to make quantitative predictions of glassy dynamics, such as the typical barriers[10] near T_g, the degree of non-exponentiality[11] and the correlation length[10] near T_g.

The escape from a given aperiodic minimum resembles the dynamics of a random field Ising magnet (RFIM) in a biasing field. The free-energy difference on a site predicted by the density functional plays the role of the magnetic field having a magnitude $TS_c(T)$. This quantity fluctuates, so the 'field' fluctuations are of the order $\sqrt{k_B T \Delta C_p}$ where ΔC_p is the configurational heat capacity of the fluctuating region. The interaction between a pair of sites in the RFIM analogy is v_{int}, which is already computed. Using this quantitative mapping, RFOT theory can predict the typical escape barrier and its fluctuations of the barriers near T_K.

The shape of a reconfiguring region is characterized by the number of contiguous sites N that are rearranged, and the number of surface interactions that are broken, b. Near T_K, the regions that dynamically reconfigure should be compact because this involves losing the smallest number of favourable interactions, b, while gaining the same configurational entropy proportional to N.

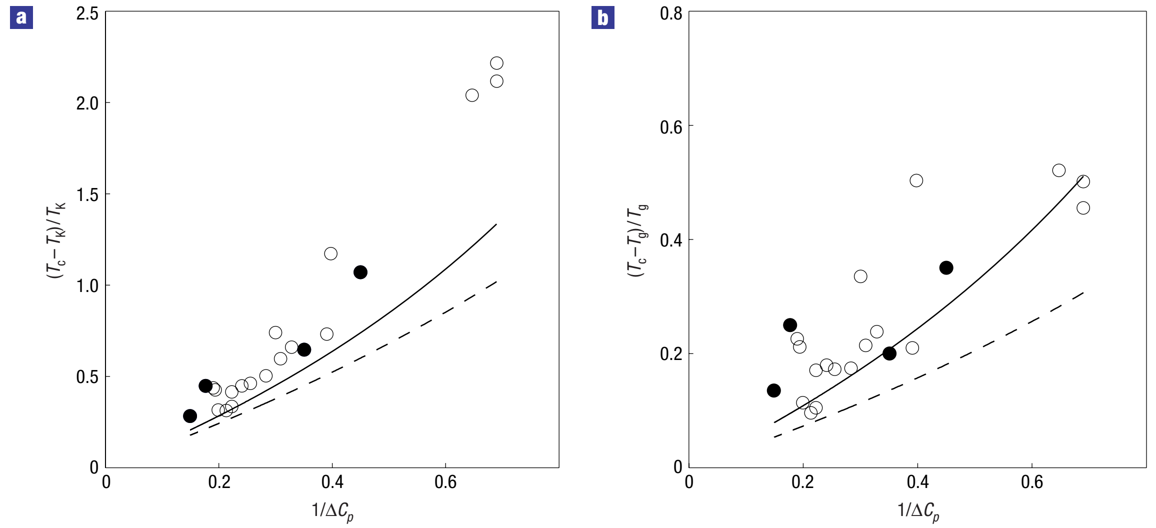

Figure 2 Predictions for the crossover temperatures. **a**, Predictions for $(T_c^{string} - T_K)/T_K$ (dashed line) and $(T_c^{perc} - T_K)/T_K$ (solid line). The experimentally derived crossover temperatures, $(T_c^{exp} - T_K)/T_K$, from Novikov and Sokolov[41], are shown as open circles with the filled circles referring to polymers. In all cases the values for the Kauzmann temperature, T_K, were taken from the correlation[48] $T_K = T_g(1 - 16/m)$. **b**, Same as for **a**, except a plot of $(T_c - T_g)/T_g$. The conversion ratio T_K/T_g was set through $S_c(T_g) = \Delta C_p(T_g - T_K)/T_K = 0.79k_B$. For both plots the ΔC_p values for the materials were determined from their m values through the correlation $m = 20.7\Delta C_p$ discussed in Stevenson and Wolynes[33].

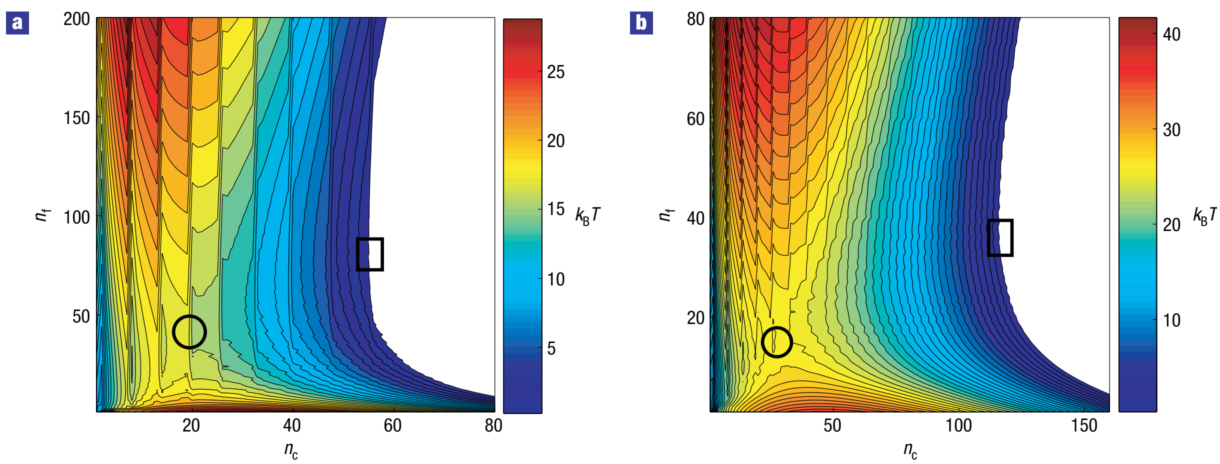

Figure 3 Free-energy contours for the fuzzy-sphere model. Two-dimensional free-energy profiles as functions of the number of particles in the core, n_c, and the number in the fuzzy halo, n_f, **a**, near T_c^{string} and **b**, near T_g. The sidebar is in units of $k_B T$ with the contour lines corresponding to intervals of $1\,k_B T$. The circles indicate the location of the typical transition state. The squares indicate a fully reconfigured region.

Maximal compactness implies a roughly spherical shape giving a free-energy cost

$$\Delta F(N) = -TS_c N + \nu_{int}\frac{z}{2}4\pi\left(\frac{N}{4\pi/3}\right)^{2/3}. \qquad (1)$$

This yields a barrier that diverges in three dimensions as S_c^{-2}. In analogy to the RFIM[31], near T_K the interface of the reconfigured region between any two aperiodic patterns will actually be wetted by other specific aperiodic minima that better match the two abutting regions than they do already. This effect lowers the surface-energy term to scale as $N^{1/2}$ rather than $N^{2/3}$. This form for the mismatch energy restores the scaling relations near T_K (ref. 9), and agrees with additional replica symmetry breaking in the interface found in replica instanton calculations[7,32]. Wetting cannot occur at short ranges, so the scale of this mismatch term still follows from ν_{int}. In this way, the observed Vogel–Fulcher scaling near T_K is predicted, $\Delta F^{\ddagger} \propto S_c^{-1}$ with the numerical proportionality coefficient depending on the microscopic value of $\nu_{int} = (1/z)(3/2)k_B T_K \log(\alpha_L/\pi e)$. The result is a universal

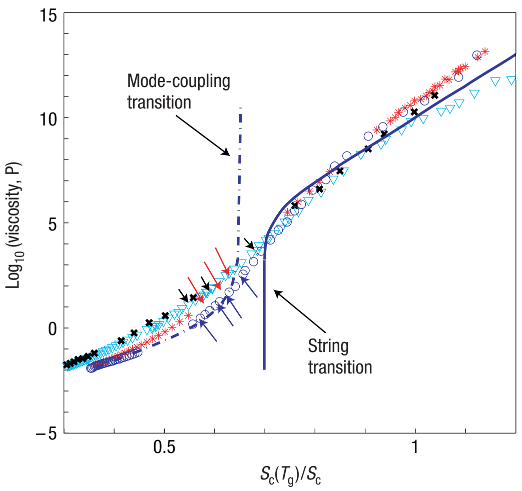

Figure 4 Predicted and experimental viscosity. A comparison of experimental viscosity with the barriers predicted from the fuzzy-sphere model (solid line). Data for salol[40], propylene carbonate[40] O-terphenyl[49,50], and alpha-phenyl-O-cresol[49,50] are represented as circles, crosses, stars and triangles respectively. An experimental mode-coupling fit to salol[44] is shown with a dot–dashed line. Experimentally derived values of the entropy at the crossover transitions[41] are shown with arrows. The free-energy barriers were placed on the $\log_{10}$(viscosity) curve by setting $\Delta F^{\ddagger}=0$ to correspond with the large T experimental value of 1 cP for the viscosity. A viscosity of 10^{10} P was used to determine the theoretical value $S_c(T_g)=0.79k_B$.

multiple of $k_B T_K$. The predicted absolute activation barriers agree well with experimental results for 44 substances[33,34], a typical deviation being less than 20%.

The compact shape of the CRR and Vogel–Fulcher behaviour are only asymptotically correct near T_K. Away from T_K, the CRR need not be compact and deviations from the Vogel–Fulcher law occur. Non-spherical shapes have an entropy advantage; although the sphere (for which $b=(z/2)4\pi(N/4\pi/3)^{2/3}$) is unique, there are many contiguous structures with other shapes. Increased temperature favours these more ramified shapes as CRRs. Contiguous shapes, called lattice animals[35], have been enumerated and play a role in problems such as percolation[36] and Yang–Lee zeros[37]. Near a spinodal of an ordinary first-order transition, the dominant nuclei should be lattice animals characteristic of clusters at the percolation threshold[24].

Accounting for the multiplicity of possible shapes, the free energy of moving a CRR of N sites with b boundary interactions is

$$\Delta F(N,b)=-TS_cN+\nu_{\rm int}b-k_BT\log(\Omega(N,b)), \qquad (2)$$

where $\Omega(N,b)$ is the number of lattice animals of given N and b, and S_c is the configurational entropy per site. For a given N the most numerous shapes are percolation-like. When these shapes dominate, we can use enumerations near the percolation limit to evaluate $\Omega(N,b)$. In percolation clusters[36], for large N,

$$\Omega_{\rm perc}(N,t)\sim\left(\frac{(\alpha+1)^{\alpha+1}}{\alpha^{\alpha}}\right)^{N}\exp\left(-\frac{N^{2\phi}}{2B^2}(\alpha-\alpha_e)^2\right). \qquad (3)$$

Here, $\alpha=t/N$, and t is the number of unoccupied sites bounding the occupied cluster. We will take the exponent, ϕ, to have its mean-field value of 1/2. B is a lattice dependent constant. $B=1.124$ (for the face centred cubic (f.c.c.) lattice) follows from fitting to numerics calculated[38] for clusters with $N\le 9$. The mean value of t/N approaches $\alpha_e=(1-p_c)/p_c$ for large N at the percolation threshold, p_c ($p_c=0.198$ for the f.c.c. lattice[38]).

To evaluate the percolation quantities required for random close packed (r.c.p.) lattices we must define a 'contact'. Spheres need not precisely touch (as in, say, percolation conductivity experiments), but intead their surfaces may be separated by at most a Lindemann length to be called connected. The parameters for this continuum percolation problem can easily be estimated because they primarily depend on the near-neighbour connectivity. The number of neighbours in the r.c.p. lattice is roughly the same as the f.c.c.; thus it is reasonable to use parameters for an f.c.c. close-packed lattice of spheres.

The number of bonds, b, is directly related to t. For the simple cubic lattice, $\langle b\rangle/\langle t\rangle=1.67$ (ref. 39), and the ratio should be linear in coordination number, z. Thus, for the r.c.p. lattice with $z=12$,

$$\Delta F(N,t)=-TS_cN+\nu_{\rm int}1.68\frac{z}{z_{\rm SC}}t-k_BT\log(\Omega_{\rm perc}(N,t)), \qquad (4)$$

where $z_{\rm SC=6}$ is the coordination number for the simple cubic lattice. To find the dominant escape route and activation barrier, we find the most probable t as a function of N. Minimizing equation (4) with respect to t, the most probable value of t is $\bar{t}=\bar{\alpha}N$, where $\bar{\alpha}=3.10$. With this most probable value, $\Omega_{\rm perc}$ becomes simply $\Omega_{\rm perc}=\lambda^N$, where $\lambda=7.64$. Each term in equation (4) is now proportional to N.

$$\Delta F(N)=k_BTN\left(-\frac{S_c}{k_B}+\frac{\nu_{\rm int}}{k_BT}1.68\frac{z_{\rm f.c.c.}}{z_{\rm SC}}\bar{\alpha}-\log\lambda\right). \qquad (5)$$

Apart from S_c, each term in this expression follows from a microscopic calculation. The free-energy profile therefore only depends on the configurational entropy, and either monotonically increases or decreases with N. If the free-energy profile increases with N, a reconfiguration event through a percolation cluster is impossible, so a more compact structure will eventually become stable for large N and provides the dominant reconfiguration route. If F decreases with N for the percolation shape, no barrier at all should be observed. The change of behaviour of $\Delta F(N)$, from increasing to decreasing with N, signals a crossover to non-activated dynamics. Introducing the $\nu_{\rm int}$ determined by RFOT yields

$$\begin{aligned}\Delta F(N)&=k_BTN\left(-\frac{S_c}{k_B}+(3.20-1.91)\right)\\&=-k_BTN\left(\frac{S_c}{k_B}-1.28\right).\end{aligned} \qquad (6)$$

Accordingly barrier-less reconfigurations occur at a critical configurational entropy, $S_c^{\rm perc}=1.28k_B$ if we neglect the mean-field softening effects on $\nu_{\rm int}$. Using the thermodynamic relation, $S_c(T)=\Delta C_p(T_g)T_g/T_K(1-T_K/T)$, RFOT theory thus yields the crossover transition temperature, $T_c^{\rm perc}$.

$$\frac{T_c^{\rm perc}}{T_K}=\left(1-\frac{S_c^{\rm perc}}{\Delta C_p}\frac{T_K}{T_g}\right)^{-1}. \qquad (7)$$

The bigger ΔC_p is, the closer $T_c^{\rm perc}$ will be to T_K; more 'fragile' liquids with larger ΔC_p have a smaller activated range, whereas a broader range for activated transport applies for stronger liquids with smaller ΔC_p. A similar trend is predicted for the mean-field crossover based on detailed microscopic calculations for fluids with a network structure[30]. The entropy at the higher mean-field crossover is $S_c(T_A)=2.0k_B$. Including the softening of $\nu_{\rm int}$ expected as this mean-field transition is approached, lowers the

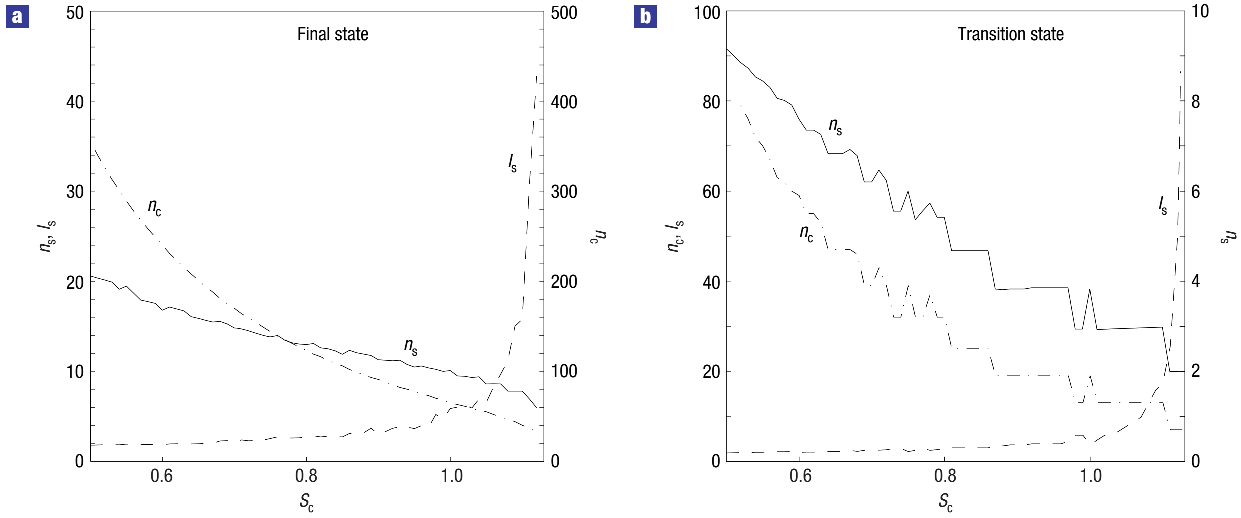

Figure 5 Shape characteristics for the fuzzy sphere. The characteristics are shown as functions of the configurational entropy for the final state and the transition state. n_c (dashed–dotted line) is the number of particles in the core, n_s (solid line) is the number of strings and l_s (dashed line) is the typical length of a string. **a**, The final state: n_c uses the axes on the right whereas n_s and l_s use the axes on the left. **b**, The transition state: here n_s uses the axes on the right whereas n_c and l_s (dashed line) use the axes on the left. The sizes and lengths are given in terms of the number of particles.

estimate of the percolation point. The amount of lowering is uncertain, however, because simultaneous with the softening, a broadening of the interface is expected, thus effectively reducing the possible entropy gain from shape fluctuations. We see that the transition occurs at the same configurational entropy level whether the liquid is fragile or strong. As in the RFOT theory of the non-exponentiality parameter β (ref. 11), fluctuations in the driving force depend on ΔC_p explicitly and should be included in equation (1). Thus, fast and slow CRRs would have somewhat different shapes (faster being more ramified generally as their entropy is higher).

Counting percolation clusters is not all that different from finding the statistics for strings. The crossover transition argument can be carried out for purely string-like objects as follows. The number of broken interactions of a string scales with length, $N(z-2)$, as does the shape entropy of a string, $\log(\Omega) = N\log(z-5)$. $(z-5)$ represents the number of directions a string can take that excludes backtracking on top of, or directly next to, the previous particle leading to a compact cluster. Using these coefficients, we find that string growth becomes down-hill at an entropy of $S_c^{\text{string}} = 1.13k_B$. The predicted crossover temperature is

$$\frac{T_c^{\text{string}}}{T_K} = \left(1 - \frac{S_c^{\text{string}}}{\Delta C_p}\frac{T_K}{T_g}\right)^{-1}, \qquad (8)$$

slightly lower than predicted by percolation. In Fig. 2a we plot the predicted T_c^{string} and T_c^{perc} versus $1/\Delta C_p$ for various liquids. Crossover temperatures from activated to non-activated dynamics were determined by using Stickel plot analysis[40]. The experimental crossover temperatures for 21 substances obtained in this way by Novikov and Sokolov[41] are plotted in the figure along with the RFOT prediction. Some of the outliers are polymers for which other slowing effects compound simple RFOT results. Uncertainty in T_K for very strong liquids is probably a source of discrepancy between the theory and experimental results for these latter substances. We also plot $(T_c - T_g)/T_g$ in Fig. 2b. According to RFOT theory, the entropy at T_g is $S_c(T_g) = \Delta C_p(T_g - T_K)/T_K = 0.79k_B$, corresponding to a glass transition at $10^{10}P$ (see Fig. 4). The quantitative agreement of the experimental crossover temperatures and the present predictions of the string and percolation transitions is striking.

To quantify the typical shapes of reconfiguring regions at temperatures between T_c and T_K, we must have a suitable analytic form of $\Omega(N,b)$ for all relevant values of N and b. Surface-roughening theories give predictions of $\Omega(N,b)$ valid for nearly spherical objects[42], but would be useful only near T_K. On the other hand, the percolation theory gives an explicit form of Ω only valid for the most populous ramified, fractal shapes that dominate near the crossover.

A reasonably effective, but unabashedly approximate, treatment of the animal-counting problem interpolates smoothly between these limits. We take the reconfiguring region to be a ‘fuzzy sphere’, a spherical core of n_c particles, surrounded by a ramified, but connected, halo of n_f particles. If we let the core size, n_c, vanish, we are only left with an extended object. Conversely, if the halo size vanishes, then we only have a sphere. The halo resembles a percolation cluster, but we will describe it as a set of strings of particles extending from the surface of the central core, because we can determine the entropic contribution of a halo of n_s strings.

Using the resulting fuzzy-sphere entropy, we can find the full-activation free-energy profile.

$$\Delta F(n_c, n_f, n_s) = \nu_{\text{int}}\frac{z}{2}\left(\frac{4\pi/3}{n_c}\right)^{1/6}\left(4\pi\left(\frac{n_c}{4\pi/3}\right)^{2/3} - n_s\right)$$
$$+\nu_{\text{int}}(z-2)n_f - TS_c(n_c+n_f) - k_B T\log(\Omega(n_c,n_f,n_s)) \qquad (9)$$

$$\Delta F(n_c, n_f) = -\log\left(\sum_{n_s}\exp(-\Delta F(n_c,n_f,n_s))\right). \qquad (10)$$

In the Supplementary Information we give the full expression for the fuzzy-sphere entropy, Ω, accounting for the excluded volume between the strings[43]. Figure 3a,b shows contour plots of the free energy at a configurational entropy value near the dynamic crossover and near the glass transition respectively. The

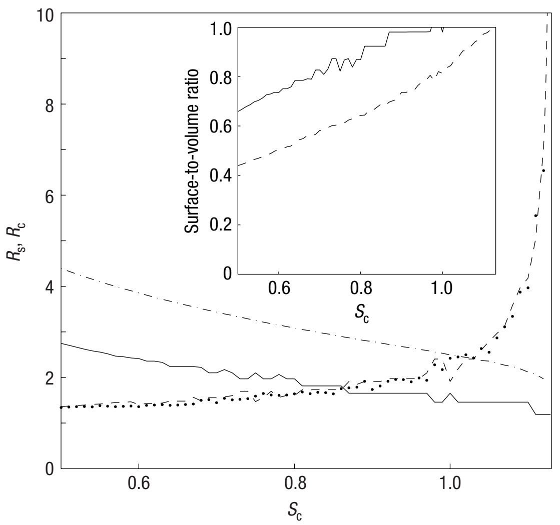

Figure 6 Radial dimensions of the fuzzy sphere. The radius of the core, R_c, at the transition state (solid line) and at the final state (dashed–dotted line). Also, the radius of the stringy halo, R_s, at the transition state (dashed line) and the final state (dotted line). The radii are given in terms of the number of particles. The inset gives the surface-to-volume ratio of the fuzzy sphere normalized to that of an infinite string. The solid line is the final state, and the dashed line is the transition state. Both plots are shown versus the configurational entropy, S_c.

saddle points on these free-energy surfaces describe transition-state ensembles for reconfiguration. The predicted barrier still depends universally on the configurational entropy as shown in Fig. 4. We also show the experimental barriers for liquids of varying fragility. The universal dependence on configurational entropy is clearly confirmed (in these plots the calorimetrically determined values of T_g were used for calibration, not the viscometric values). At low T, the barrier clearly depends linearly on $1/S_c$ for $S_c < S_c^{\text{string}}$, consistent with the asymptotic RFOT analysis, but as the critical value of the configurational entropy, S_c^{string}, is approached the activation barrier rapidly decreases, dropping to zero at S_c^{string}. The experimental mode-coupling fit to the viscosity[44] shows a striking symmetry. The mode-coupling theory fits the dynamic transition from above, whereas the current argument predicts its emergence from below.

The shapes of CRRs are broadly distributed as shown in the broad $1k_BT$ contour in the plots. Examples of the final shape expected near T_g and near the crossover temperature are shown in Fig. 1. To specifically quantify the characteristic final shape, we take it to be the one with the smallest core. Figures 5 and 6 show how the resulting scales of the transition states and CRRs change with configurational entropy. Near T_g, the shapes are mostly spherical with just a small fraction of the particles in the stringy halo. This size agrees with the previous Xia–Wolynes estimate. They consist of around 125 particles (beads) near T_g, and are thus bigger than the CRRs invoked in the venerable Adam–Gibbs approach[45]. This prediction of RFOT theory received dramatic confirmation in an experimental study by Berthier *et al.*[46]. They show that multi-point correlations near T_g correspond to a correlation length of about 5 units, independent of fragility. A typical protuberance on the compact core near T_g contains only two particles. Near T_c^{string}, however, the core size becomes very small, and the strings lengthen dramatically. This growth occurs for both the transition state and the final state. A powerful probe that should be able to determine the shape of the CRRs is a version of the spin-diffusion nuclear magnetic resonance experiment of Tracht *et al.*[47]. The spin diffusion between neighbouring slow and fast regions directly measures the surface-to-volume ratio, which changes as the CRRs change from compact to stringy. We show our prediction of this ratio in the inset of Fig. 6.

The string lengths near T_c^{string} are larger than those usually reported in simulations or in microscopy. This apparent discrepancy arises from a kinetic effect as follows: although the free-energy barrier for creating a string approaches zero at T_c^{string}, the actual time to construct a string grows with the length of the string. The barrier to create a new string is somewhat larger than that to extend an old one. Because of this, the growth/death of a string takes place particle-by-particle on the microscopic timescale, and should be diffusive, with growth time $\tau_s = \tau^0_{\text{micro}} l_s^2$. Here, τ^0_{micro} is a typical vibrational timescale, that is, the time for a particle to explore its cage. When τ_s becomes comparable to the time for another activated event to occur in the immediate vicinity of the string, τ_α / l_s, the growth of the original string will be interrupted. Here, $\tau_\alpha = \tau^0_{\text{micro}} e^{F^\ddagger/k_B T}$. This finite growth time gives a maximum limit for the length of strings:

$$l^3_{s,\max} = e^{F^\ddagger/k_B T}. \quad (11)$$

Larger strings will be interrupted, or 'incoherent', as an activated event occurs along the string. This phenomenon of 'incoherent' strings is seen in simulations[18]. Using the fuzzy-sphere model, the minimum barrier corresponds to a core region with seven particles. This gives an $F^\ddagger$ consistent with what Novikov and Sokolov[41] call the 'magic' relaxation time for the crossover and a length $l_{s.\max} \cong e^{14/3} \cong 108$. Although larger than the lengths usually quoted from simulations, the rapid variation of $F^\ddagger$ and l_s near the string transition makes this result rather sensitive to modelling details. The key is that there is a natural cut-off of kinetic origin that causes T_c^{string} to be a crossover and not a sharp transition.

We see that the random first-order transition theory predicts that CRRs are compact, nearly spherical objects in the deep supercooled region, but that in the moderately supercooled region, near the mode-coupling transition, the CRRs become non-compact, extended string-like objects. The crossover temperature is entropically controlled, allowing the prediction of the dynamic crossover temperature. This result is confirmed experimentally.

Received 21 July 2005; accepted 21 February 2006; published 26 March 2006.

References

1. Singh, Y., Stoessel, J. P. & Wolynes, P. G. Hard-sphere glass and the density-functional theory of aperiodic crystals. *Phys. Rev. Lett.* **54,** 1059–1062 (1985).
2. Kirkpatrick, T. R. & Wolynes, P. G. Connections between some kinetic and equilibrium theories of the glass transition. *Phys. Rev. A* **35,** 3072–3080 (1987).
3. Kirkpatrick, T. R. & Wolynes, P. G. Stable and metastable states in mean-field potts and structural glasses. *Phys. Rev. B* **36,** 8552–8564 (1987).
4. Kirkpatrick, T. R. & Thirumalai, D. Dynamics of the structural glass-transition and the p-spin-interaction spin-glass model. *Phys. Rev. Lett.* **58,** 2091–2094 (1987).
5. Mezard, M. & Parisi, G. Thermodynamics of glasses: A first principles computation. *Phys. Rev. Lett.* **82,** 747–750 (1999).
6. Franz, S. & Toninelli, F. L. A field-theoretical approach to the spin glass transition: models with long but finite interaction range. *J. Stat. Mech. Theor. Exp.* P01008 (2005).
7. Franz, S. Metastable states, relaxation times and free-energy barriers in finite dimensional glassy systems. *Europhys. Lett.* **73,** 492–498 (2005).
8. Bouchaud, J. P. & Biroli, G. On the Adam-Gibbs-Kirkpatrick-Thirumalai-Wolynes scenario for the viscosity increase in glasses. *J. Chem. Phys.* **121,** 7347–7354 (2004).
9. Kirkpatrick, T. R., Thirumalai, D. & Wolynes, P. G. Scaling concepts for the dynamics of viscous liquids near an ideal glassy state. *Phys. Rev. A* **40,** 1045–1054 (1989).
10. Xia, X. Y. & Wolynes, P. G. Fragilities of liquids predicted from the random first order transition theory of glasses. *Proc. Natl Acad. Sci.* **97,** 2990–2994 (2000).
11. Xia, X. Y. & Wolynes, P. G. Microscopic theory of heterogeneity and nonexponential relaxations in supercooled liquids. *Phys. Rev. Lett.* **86,** 5526–5529 (2001).
12. Ediger, M. D. Spatially heterogeneous dynamics in supercooled liquids. *Ann. Rev. Phys. Chem.* **51,** 99–128 (2000).
13. Russell, E. V. & Israeloff, N. E. Direct observation of molecular cooperativity near the glass transition. *Nature* **408,** 695–698 (2000).
14. Deschenes, L. A. & Bout, D. A. V. Single-molecule studies of heterogeneous dynamics in polymer melts near the glass transition. *Science* **292,** 255–258 (2001).
15. Sillescu, H. Heterogeneity at the glass transition: a review. *J. Non-Cryst. Solids* **243,** 81–108 (1999).
16. Richert, R. Heterogeneous dynamics in liquids: fluctuations in space and time. *J. Phys. Condens. Matter* **24,** R703–R738 (2002).

17. Kob, W., Donati, C., Plimpton, S. J., Poole, P. H. & Glotzer, S. C. Dynamical heterogeneities in a supercooled Lennard-Jones liquid. *Phys. Rev. Lett.* **79,** 2827–2830 (1997).
18. Gebremichael, Y., Vogel, M. & Glotzer, S. C. Particle dynamics and the development of string-like motion in a simulated monoatomic supercooled liquid. *J. Chem. Phys.* **120,** 4415–4427 (2004).
19. Donati, C. *et al.* Stringlike cooperative motion in a supercooled liquid. *Phys. Rev. Lett.* **80,** 2338–2341 (1998).
20. Donati, C., Glotzer, S. C., Poole, P. H., Kob, W. & Plimpton, S. J. Spatial correlations of mobility and immobility in a glass-forming Lennard-Jones liquid. *Phys. Rev. E* **60,** 3107–3119 (1999).
21. Weeks, E. R., Crocker, J. C., Levitt, A. C., Schofield, A. & Weitz, D. A. Three-dimensional direct imaging of structural relaxation near the colloidal glass transition. *Science* **287,** 627–631 (2000).
22. Reinsberg, S. A., Heuer, A., Doliwa, B., Zimmermann, H. & Spiess, H. W. Comparative study of the nmr length scale of dynamic heterogeneities of three different glass formers. *J. Non-Cryst. Solids* **307–310,** 208–214 (2002).
23. Biroli, G. & Bouchaud, J. P. Diverging length scale and upper critical dimension in the mode-coupling theory of the glass transition. *Europhys. Lett.* **67,** 21–27 (2004).
24. Unger, C. & Klein, W. Nucleation theory near the classical spinodal. *Phys. Rev. B* **29,** 2698–2708 (1984).
25. Johnson, G., Mel'cuk, A. I., Gould, H., Klein, W. & Mountain, R. D. Molecular-dynamics study of long-lived structures in a fragile glass-forming liquid. *Phys. Rev. E* **57,** 5707–5718 (1998).
26. Stoessel, J. P. & Wolynes, P. G. Linear excitations and the stability of the hard-sphere glass. *J. Chem. Phys.* **80,** 4502–4512 (1984).
27. Dasgupta, C. & Valls, O. T. Free energy landscape of a dense hard-sphere system. *Phys. Rev. E* **59,** 3123–3134 (1999).
28. Fuchizaki, K. & Kawasaki, K. Dynamical density functional theory for glassy behaviour. *J. Phys. Condens. Matter* **14,** 12203–12222 (2002).
29. Stillinger, F. H. & Weber, T. A. Dynamics of structural transitions in liquids. *Phys. Rev. A* **28,** 2408–2416 (1983).
30. Hall, R. W. & Wolynes, P. G. Microscopic theory of network glasses. *Phys. Rev. Lett.* **90,** 085505 (2003).
31. Villain, J. Equilibrium critical properties of random field systems — new conjectures. *J. Physique* **46,** 1843–1852 (1985).
32. Dzero, M., Schmalian, J. & Wolynes, P. G. Activated events in glasses: The structure of entropic droplets. *Phys. Rev. B* **72,** 100201 (2005).
33. Stevenson, J. D. & Wolynes, P. G. Thermodynamic-kinetic correlations in supercooled liquids: A critical survey of experimental data and predictions of the random first-order transition theory of glasses. *J. Phys. Chem. B* **109,** 15093–15097 (2005).
34. Lubchenko, V. & Wolynes, P. G. Barrier softening near the onset of nonactivated transport in supercooled liquids: Implications for establishing detailed connection between thermodynamic and kinetic anomalies in supercooled liquids. *J. Chem. Phys.* **119,** 9088–9105 (2003).
35. Stauffer, D. Monte-carlo study of density profile, radius, and perimeter for percolation clusters and lattice animals. *Phys. Rev. Lett.* **41,** 1333–1336 (1978).
36. Leath, P. L. Cluster size and boundary distribution near percolation threshold. *Phys. Rev. B* **14,** 5046–5055 (1976).
37. Yang, C. N. & Lee, T. D. Statistical theory of equations of state and phase transitions. I Theory of condensation. *Phys. Rev.* **87,** 404–409 (1952).
38. Sykes, M. F., Gaunt, D. S. & Glen, M. Percolation processes in three dimensions. *J. Phys. A* **9,** 1705–1712 (1976).
39. Cao, Q. Z. & Wong, P. O. External surface of site percolation clusters in three dimensions. *J. Phys. A* **25,** L69–L74 (1992).
40. Stickel, F., Fischer, E. W. & Richert, R. Dynamics of glass-forming liquids. 2. detailed comparison of dielectric relaxation, dc-conductivity, and viscosity data. *J. Chem. Phys.* **104,** 2043–2055 (1996).
41. Novikov, V. N. & Sokolov, A. P. Universality of the dynamic crossover in glass-forming liquids: A 'magic' relaxation time. *Phys. Rev. E* **67,** 031507 (2003).
42. Chui, S. T. & Weeks, J. D. Phase-transition in 2-dimensional Coulomb gas, and interfacial roughening transition. *Phys. Rev. B* **14,** 4976–4982 (1976).
43. Flory, P. J. *Principles of Polymer Chemistry* (Cornell Univ. Press, Ithaca, 1953).
44. Hinze, G., Brace, D. D., Gottke, S. D. & Fayer, M. D. A detailed test of mode-coupling theory on all time scales: Time domain studies of structural relaxation in a supercooled liquid. *J. Chem. Phys.* **113,** 3723–3733 (2000).
45. Adam, G. & Gibbs, J. H. On the temperature dependence of cooperative relaxation properties in glass-forming liquids. *J. Chem. Phys.* **43,** 139–146 (1943).
46. Berthier, L. *et al.* Direct experimental evidence of a growing length scale accompanying the glass transition. *Science* **310,** 1797–1800 (2005).
47. Tracht, U. *et al.* Length scale of dynamic heterogeneities at the glass transition determined by multidimensional nuclear magnetic resonance. *Phys. Rev. Lett.* **81,** 2727–2730 (1998).
48. Böhmer, R. & Angell, C. A. Correlations of the nonexponentiality and state dependence of mechanical relaxations with bond connectivity in Ge-As-Se supercooled liquids. *Phys. Rev. B* **45,** 10091–10094 (1992).
49. Laughlin, W. T. & Uhlmann, D. R. Viscous flow in simple organic liquids. *J. Phys. Chem.* **76,** 2317–2325 (1972).
50. Cukierman, M., Lane, J. W. & Uhlmann, D. R. High-temperature flow behavior of glass-forming liquids: A free-volume interpretation. *J. Chem. Phys.* **59,** 3639–3644 (1973).

Acknowledgements

Work at UCSD was supported by NSF grant CHE0317017. J.S. was supported by the Ames Laboratory, operated for the US Department of Energy by Iowa State University under Contract No. W-7405-Eng-82 (J.S.). We would also like to acknowledge K. Schmidt-Rohr for helpful comments.
Correspondence and requests for materials should be addressed to P.G.W.
Supplementary Information accompanies this paper on www.nature.com/naturephysics.

Competing financial interests

The authors declare that they have no competing financial interests.